



**CIMNE. International Centre for Numerical Methods in Engineering**

**Master of Science in Computational Mechanics**

**Universitat Politècnica de Catalunya**

**Computational Solid Mechanics**

**Assignment #1**

**Submitted By**

**Aly Youssef**

**13/4/2018**

## TABLE OF CONTENTS

|   |    |
|---|----|
| Introduction .....  | 4  |
| 1- Inviscid model .....   | 4  |
| 1-1 Elastic domain model.....   | 4  |
| 1-2 Hardening law .....   | 5  |
| 1-3 Assessing the correctness of the implementation .....                       | 6  |
| 1-3-1 First case: Uniaxial tension-compression-tension loading .....            | 6  |
| 1-3-2 Second case: Uniaxial tension - biaxial compression-tension loading ..... | 8  |
| 2- Viscous (rate dependent) model .....   | 13 |
| 2-1 Assessing the correctness of the implementation .....                       | 13 |
| 2-2-1 Variation of the viscosity parameter $\eta$ .....                         | 13 |
| 2-2-2 Variation of the strain rate $\dot{\epsilon}$ .....                       | 14 |
| 2-2-3 Variation of the time integration parameter $\alpha$ .....                | 14 |
| 2-2 Tangent and algorithmic constitutive operators <b>C11</b> .....             | 15 |
| Appendix .....  | 17 |
| Appendix 1-1 .....  | 17 |
| Appendix 1-2 .....  | 17 |
| Appendix 2-1 .....  | 17 |
| Appendix 2-2 .....  | 18 |

## List of figures

|   |    |
|---|----|
| Figure 1: Tension only elastic domain model .....   | 4  |
| Figure 2: Non-symmetric elastic domain model .....  | 5  |
| Figure 3: Internal variable (r) vs. hardening parameter (q) .....                                   | 5  |
| Figure 4: Stress vs. strain for the symmetric damage surface .....                                  | 6  |
| Figure 5: internal variable (r) vs. time for the symmetric model.....                               | 6  |
| Figure 6: Stress vs. strain for the tension only damage surface .....                               | 7  |
| Figure 7: internal variable (r) vs. time for the tension only model.....                            | 7  |
| Figure 8: Stress vs. strain for the non-symmetric damage surface .....                              | 7  |
| Figure 9: internal variable (r) vs. time for the non-symmetric model .....                          | 8  |
| Figure 10: Stress vs. strain for the symmetric damage surface in the $\sigma_1$ direction.....      | 8  |
| Figure 11: Stress vs. strain for the symmetric damage surface in the $\sigma_2$ direction .....     | 9  |
| Figure 12: internal variable (r) vs. time for the symmetric model.....                              | 9  |
| Figure 13: Stress vs. strain for the tension only damage surface in the $\sigma_1$ direction.....   | 9  |
| Figure 14: Stress vs. strain for the tension only damage surface in the $\sigma_2$ direction.....   | 10 |
| Figure 15: Stress vs. strain for the non-symmetric damage surface in the $\sigma_1$ direction.....  | 10 |
| Figure 16: Stress vs. strain for the non-symmetric damage surface in the $\sigma_2$ direction ..... | 10 |
| Figure 17: Stress vs. strain for the symmetric damage surface .....                                 | 11 |
| Figure 18: Hardening parameter(q) vs. time for the symmetric model (case 1 and case 3) .....        | 11 |
| Figure 19: Stress vs. strain for the tension only damage surface .....                              | 11 |
| Figure 20: Stress vs. strain for the non-symmetric damage surface .....                             | 12 |
| Figure 21: Stress vs. strain curves for $\eta = 1, 0.8, 0.4$ and $0$ .....                          | 13 |
| Figure 22: Stress strain curve for the same input parameters for the inviscid model .....           | 13 |
| Figure 23: Stress vs. time for $\eta = 0$ and $1$ .....   | 14 |
| Figure 24: Stress vs. strain curve for different strain rates.....                                  | 14 |
| Figure 25: Stress vs. strain for $\alpha = 0, 0.5$ and $1$ .....                                    | 15 |
| Figure 26: Constitutive algorithmic/tangent tensor vs. time for $\alpha = 0, 0.5$ and $1$ .....     | 16 |

## INTRODUCTION

This report handles the topic of continuum damage models applied in the context of solid mechanics. Such a model is implemented in order to mimic the material's loss of stiffness. Such a phenomenon is due to the dislocation motion and other microscopic phenomenon that occur inside the material once it exceeds its elastic limit. Such model could be used in order to simulate such effects on a continuum scale. The model could either capture hardening or softening behavior; however, for the majority of practical applications, a softening behavior is predominate used.

The report in hand focuses on implementing and assessing the correctness of damage models, namely the inviscid and viscous damage models, on a Gauss point level. Such models are developed through the modification of a supplied MATLAB code. As an initial step, the strains exerted on the material are inserted into the code through a loading path in the principal stress space that is pre-prescribed by the user. Depending on the implemented model and its parameters the results are then obtained.

### 1- INVISCID MODEL

The first section of this report handles the implementation and evaluation of the correctness of the inviscid damage model. In such a model, the effect of the viscosity is neglected thus eliminating the dependency of the results and behavior on the rate at which the loads are applied. Regarding the implementation of the model, several modifications were added to the provided code. As a first addition, different models for the elastic domain were applied: non-symmetric and tension only elastic domain models. The second addition is the implementation of the exponential hardening/softening law.

#### 1-1 Elastic domain model

The implementation of the tension only elastic domain model is shown in Figure 1 (see Appendix 1-1 for the code). The main characteristics of such model could be observed in the result. The damage surface delimits the elastic region only in positive quadrants of the principal stresses (i.e. tension). Beyond such limits damage is expected to occur. However, no such limits exist in the negative quadrants (i.e. compression) of the principal stresses as the damage surface tends to infinity. Thus, damage does not occur in the material when subjected to compressive stresses.

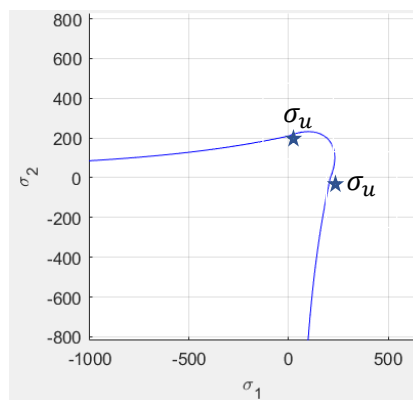


Figure 1: Tension only elastic domain model

The implementation of the tension only elastic domain model is shown in Figure 2 (see Appendix 1-1 for the code)Figure 1. The main characteristics of such model could be observed in the result. A ratio exists between the limits in the tension and compression sides of the damage surface. In the case of this

implementation the applied ratio is 3. Thus, the stress limit beyond which damage occurs is 3 times larger in compression than in tension.

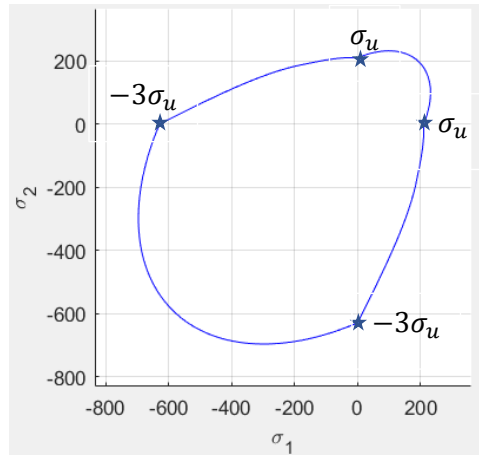


Figure 2: Non-symmetric elastic domain model

## 1-2 Hardening law

The second addition to the code is the implementation of an exponential hardening/softening law (see Appendix 1-2 for the code). In order to access the correctness of the implementation. The internal variable  $r$  is plotted against the hardening parameter  $q$  in Figure 3 for the case of a positive hardening parameter  $H$ . This plot was obtained by applying a uniaxial tensile stress. It could be seen that an exponential behavior is expressed. Hardening is initialized at a given slope  $H$  which decreases exponentially until a value of almost zero is reached at infinity.

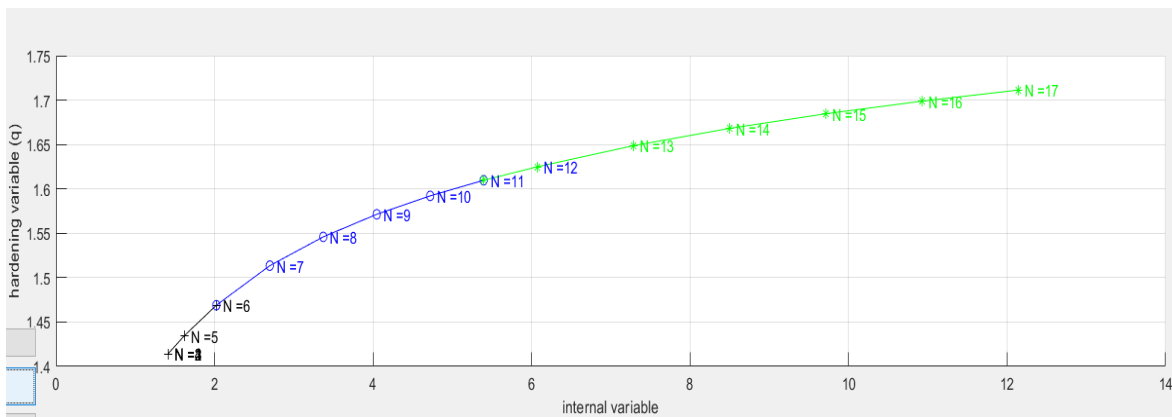


Figure 3: Internal variable ( $r$ ) vs. hardening parameter ( $q$ )

### 1-3 Assessing the correctness of the implementation

The material parameters used for all three cases are as follows:  $H = -0.2$ ,  $\nu = 0.3$  and  $E = 2000$ .

#### 1-3-1 First case: Uniaxial tension-compression-tension loading

In the first case, uniaxial stress is exerted on the material. This is to be applied for the tension only and non-symmetric elastic damage surfaces. A tensile phase is applied initially to the point where damage would occur. This is followed by a compressive phase until damage occurs again (damage condition only applicable for the non-symmetric case). Then this is followed by another tensile phase until damage is achieved once again. The values used for the stress are as follows:

$$\Delta\sigma_1^{(1)} = 400; \Delta\sigma_1^{(2)} = -1200; \Delta\sigma_1^{(3)} = 2000 \text{ and } \Delta\sigma_1^{(1,2,3)} = 0$$

The result for the stress vs. the strain, in the direction of the applied stresses, for the symmetric model is plotted in Figure 4 as a reference for the analysis. The initial tensile phase in black is followed by a compressive phase in blue which is followed by another tensile phase in green (a similar pattern is carried out in the following two cases). It could be seen that all the phases reach a damaged state where a decreasing linear behavior is expressed (negative hardening parameter). It could be noted that both the black and blue phases reach the same stress levels as the model is symmetrical. It could be also noted that due to the occurrence of damage, the damage surface has shrunk thus the slopes at which the elastic behavior occurs is different from original one. This entails that the material will not follow the same path for when in the elastic range once damage has occurred.

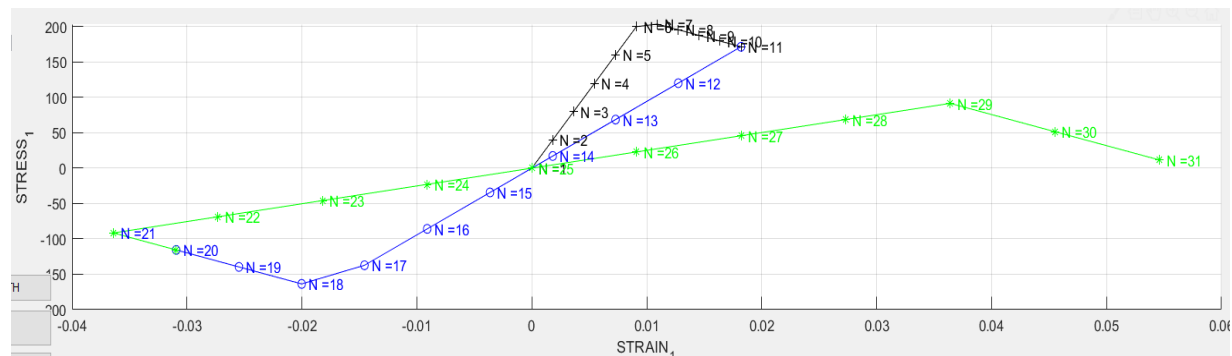


Figure 4: Stress vs. strain for the symmetric damage surface

Figure 5 further confirms that occurrence of damage in the three phases signaled by the increase of the internal parameter.

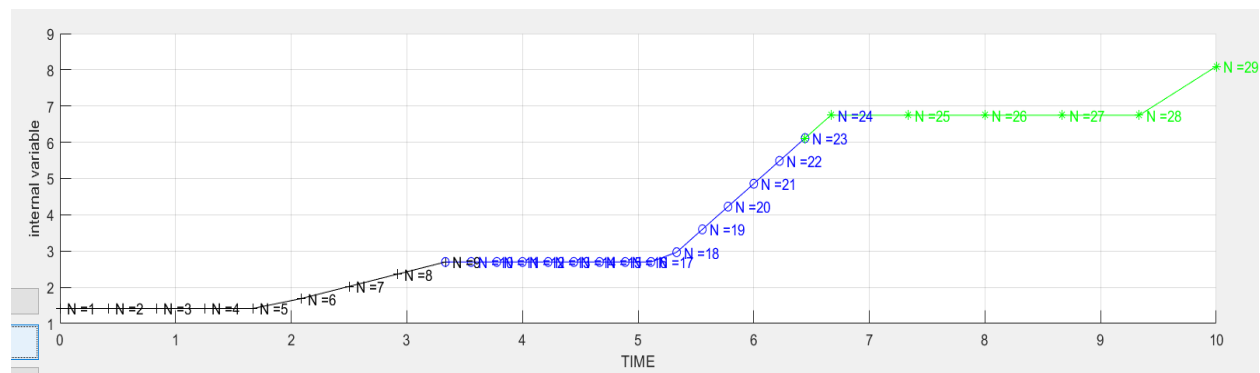


Figure 5: internal variable (r) vs. time for the symmetric model

The tension only model is shown in Figure 6. It could be seen that the behavior of the initial tension phase in black is similar to the behavior that occurs in the symmetric model. However, it could be noted that the compressive phase in blue (overlaid by the green curve) exhibits a compressive behavior only without the occurrence of any damage.

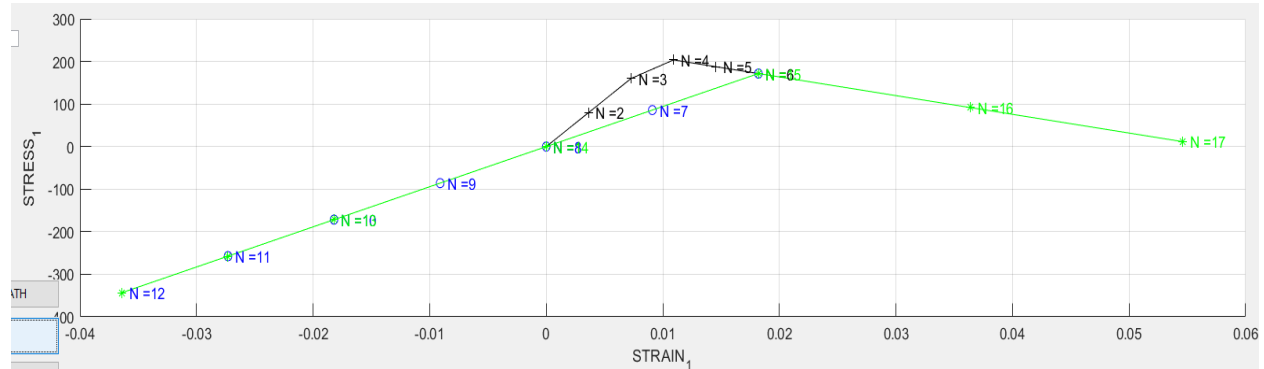


Figure 6: Stress vs. strain for the tension only damage surface

Figure 7 further confirms that occurrence of damage in the tensile phases only signaled by the increase of the internal parameter where in the compressive phase no increase has occurred.

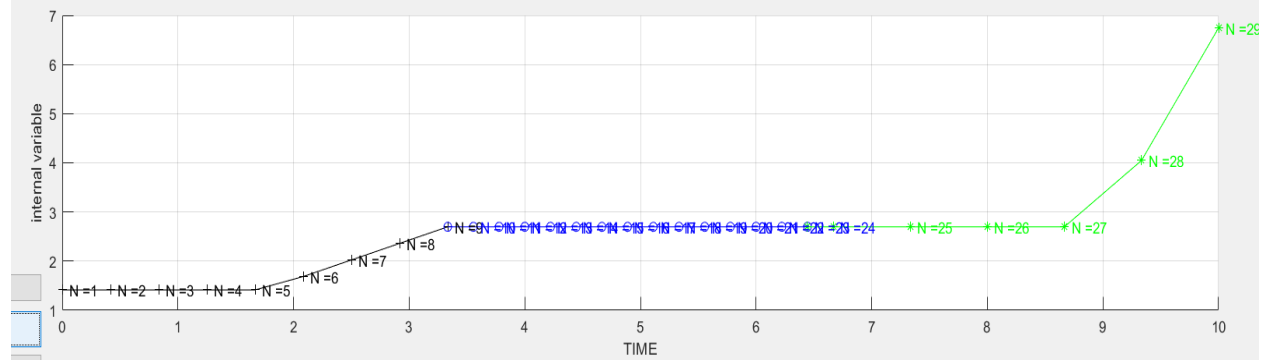


Figure 7: internal variable (r) vs. time for the tension only model

The non-symmetric model is shown in Figure 8. A ratio of 1.5 was used in order to ensure that damage occurs for all phases using the prescribed stresses. It could be seen that a similar behavior to the symmetric model occurs. However, the value for the onset of damage in the blue compressive phase is 1.5 times larger than the one in the symmetric model. This is due to the non-symmetry of the behavior of the material in tension compared to tension.

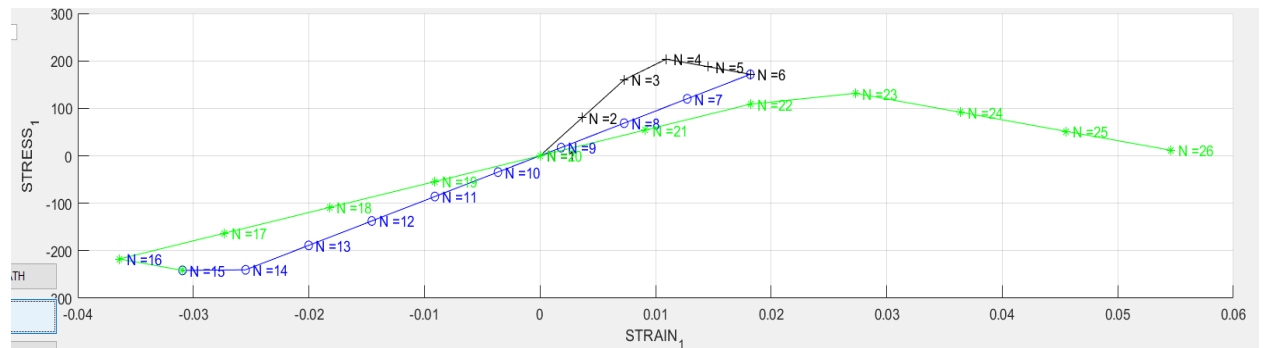


Figure 8: Stress vs. strain for the non-symmetric damage surface

Figure 9 Figure 5 further confirms that occurrence of damage in the three phases signaled by the increase of the internal parameter. However, the values are different from those obtained using the symmetric model due to the non-symmetry between tension and compression.

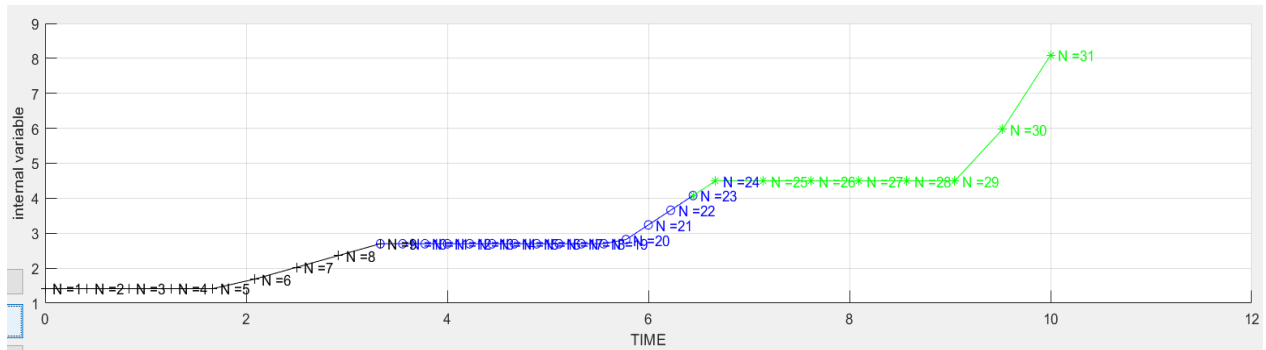


Figure 9: internal variable (r) vs. time for the non-symmetric model

### 1-3-2 Second case: Uniaxial tension - biaxial compression-tension loading

In the second case, biaxial stress is exerted on the material. The model implementation is similar to the first case. The values used for the stress are as follows:

$$\Delta\sigma_1^{(1)} = 500, \Delta\sigma_1^{(2)} = 0; \Delta\sigma_1^{(2)} = \Delta\sigma_2^{(2)} = -900; \Delta\sigma_1^{(3)} = \Delta\sigma_1^{(3)} = 1800.$$

The result for the stress vs. the strain, in the direction of the applied stresses, for the symmetric model is plotted in Figure 10 and Figure 11, for the  $\sigma_1$  and  $\sigma_2$  direction respectively, as a reference for the analysis. All three phases of the loading are subjected to damage as shown in Figure 12 which is signaled by the increase in the internal parameter r. It is worth nothing that the behavior in the  $\sigma_1$  direction is different from the  $\sigma_2$  direction due to the nature of the prescribed stresses. The stresses in the  $\sigma_1$  direction increase in the tension phases (black and green lines) while it decreases in the compressive phase (blue line). The same could be said for the  $\sigma_2$  direction; however, in the initial tensile phase, the strain decreases at constant stress. This is due to the Poisson's effect in the material. Another expression of the Poisson's effect is that the value of stress does not pass through the origin while in the compressive phase in the  $\sigma_1$  direction.

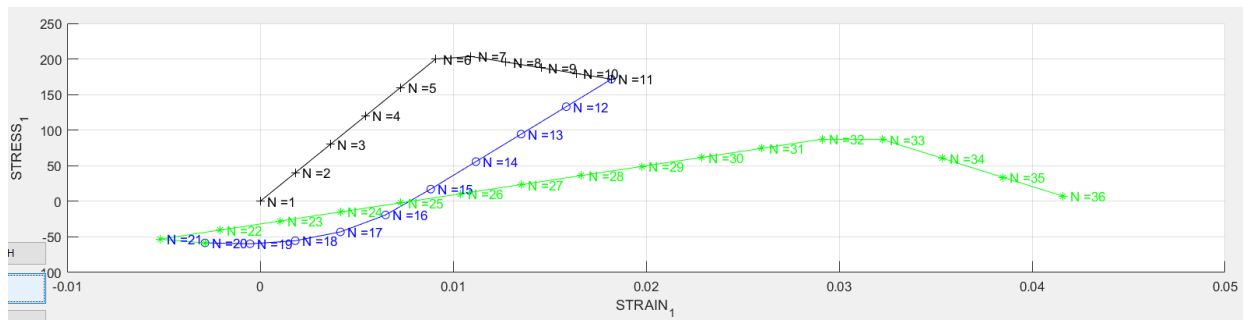


Figure 10: Stress vs. strain for the symmetric damage surface in the  $\sigma_1$  direction

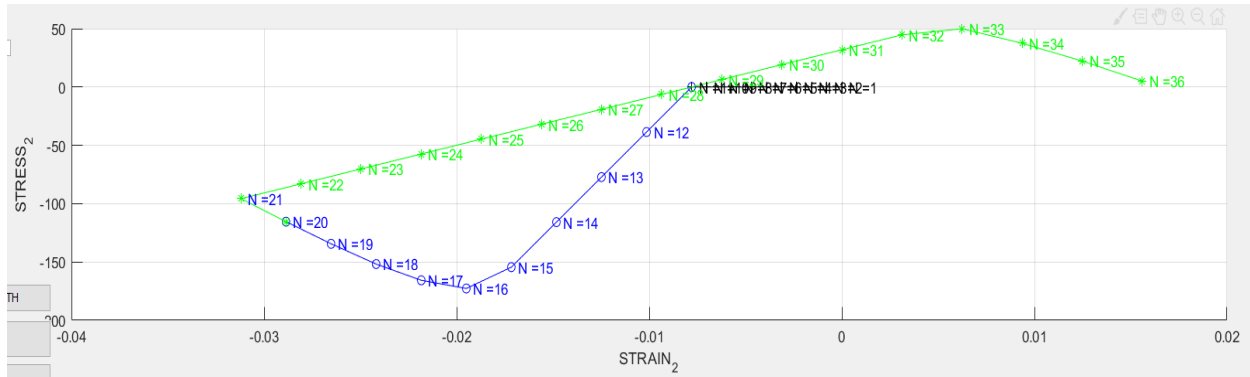


Figure 11: Stress vs. strain for the symmetric damage surface in the  $\sigma_2$  direction

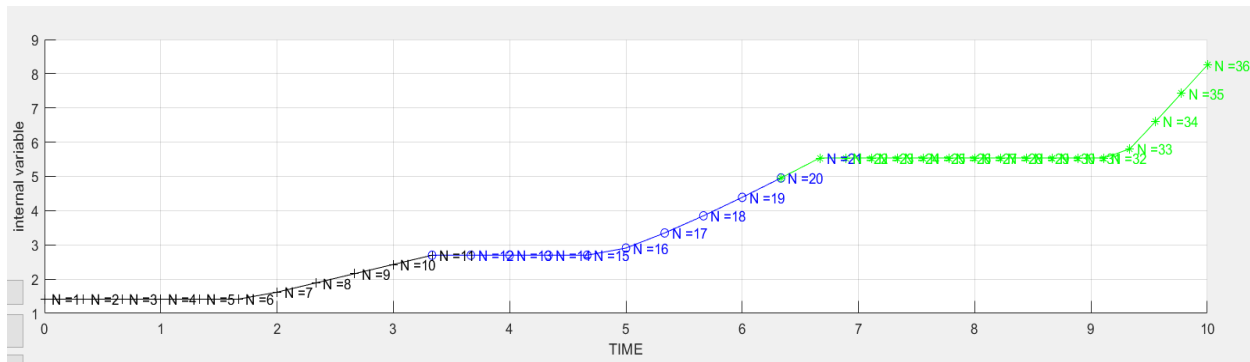


Figure 12: internal variable ( $r$ ) vs. time for the symmetric model

The result for the stress vs. the strain, in the direction of the applied stresses, for the tension only model is plotted in Figure 13 and Figure 14, for the  $\sigma_1$  and  $\sigma_2$  direction respectively. It could be seen that the behavior of the tensile phases in the  $\sigma_1$  direction (black and green curves) is similar to the behavior that occurs in the symmetric model. However, it could be noted that the compressive phase (blue curve overlaid by the green curve) exhibits solely a compressive behavior without any damage. The initial tensile phase in the  $\sigma_2$  direction exhibits a reduction in strain at constant stress due to the effect of the Poisson's ratio.

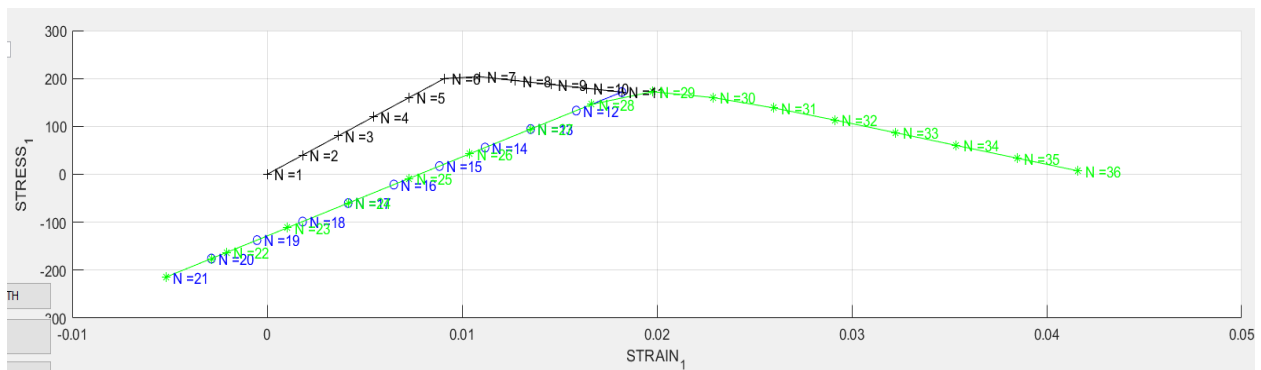


Figure 13: Stress vs. strain for the tension only damage surface in the  $\sigma_1$  direction

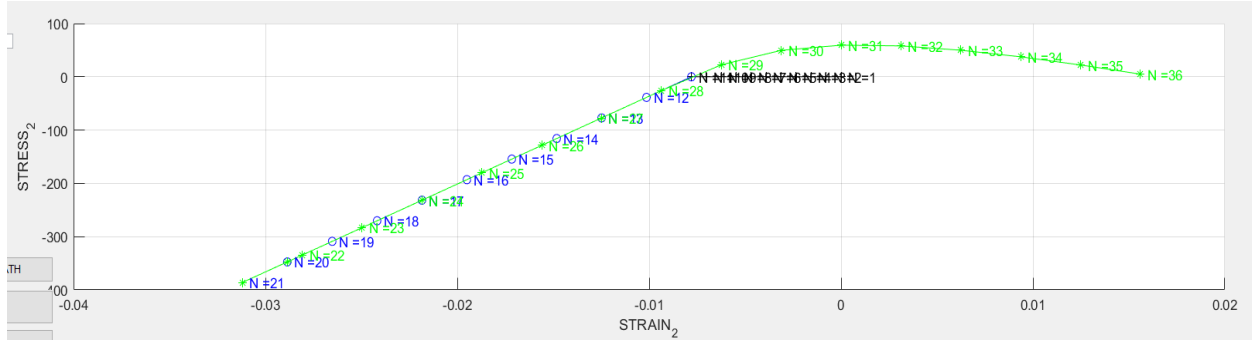


Figure 14: Stress vs. strain for the tension only damage surface in the  $\sigma_2$  direction

The result for the stress vs. the strain, in the direction of the applied stresses, for the non-symmetric model is plotted in Figure 15 and Figure 16, for the  $\sigma_1$  and  $\sigma_2$  direction respectively. A similar setup was used as in case 1. It could be seen that a similar behavior to the symmetric model occurs. However, the value for the onset of damage in the blue compressive phase is 1.5 times larger than the one in the symmetric model. This is due to the non-symmetry of the behavior of the material in tension compared to tension. Again, the initial tensile phase in the  $\sigma_2$  direction exhibits a reduction in strain at constant stress due to the effect of the Poisson's ratio.

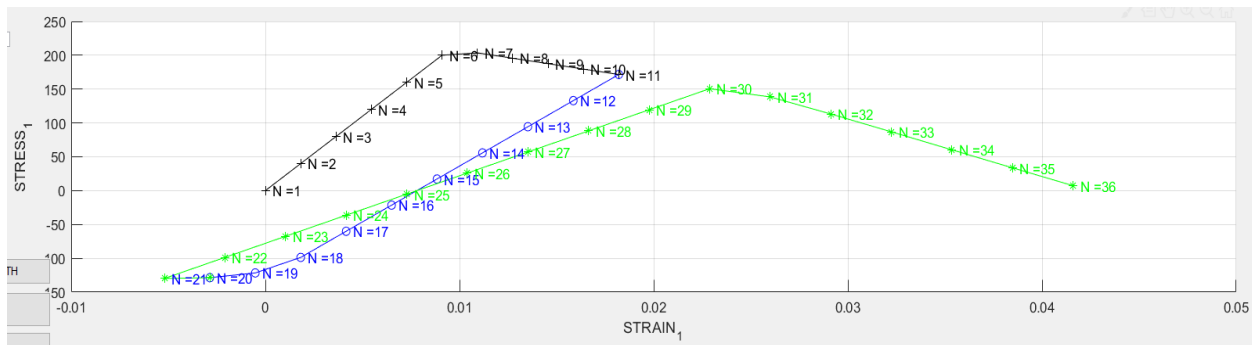


Figure 15: Stress vs. strain for the non-symmetric damage surface in the  $\sigma_1$  direction

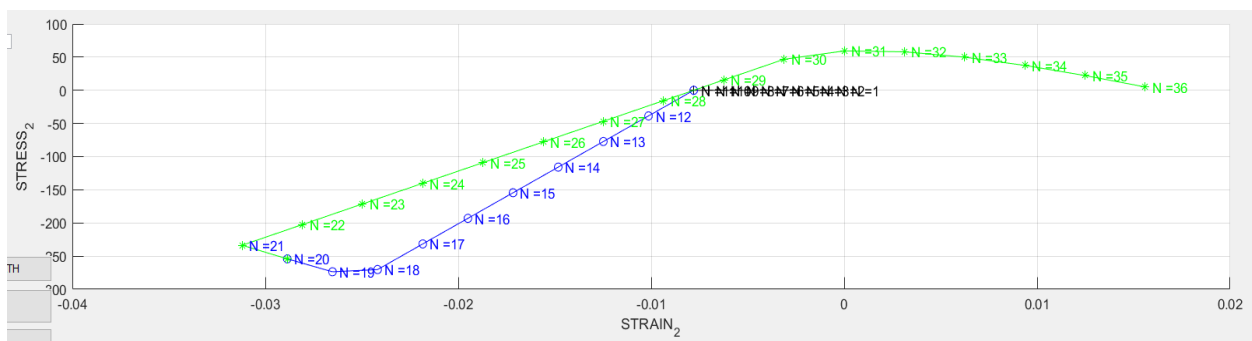


Figure 16: Stress vs. strain for the non-symmetric damage surface in the  $\sigma_2$  direction

### 1-3-3 Third case: Biaxial tension-compression-tension loading

In the third case, uniaxial stress is exerted on the material followed by a biaxial stress. The model implementation is similar to the first case. The values used for the stress are as follows:

$$\Delta\sigma_1^{(1)} = \Delta\sigma_2^{(1)} = 400; \Delta\sigma_1^{(2)} = \Delta\sigma_2^{(2)} = -1200; \Delta\sigma_1^{(3)} = \Delta\sigma_2^{(3)} = 2000.$$

The result for the stress vs. the strain in the  $\sigma_1$  direction for the symmetric model is plotted in Figure 17 as a reference for the analysis. The results for  $\sigma_1$  and  $\sigma_2$  are identical due to the linear nature of the applied stresses. It could be observed that the behavior is similar to the one obtained in case 1. However, the effect of softening is more pronounced in case 2. This is shown through Figure 18 where case 2 follows a curve with smaller value compared to case 1. This is due to the fact that the material is stretched in both axes hence increasing the amount of energy it is subjected to. The loading/unloading curve passes through the origin as the deformation equal in both directions. This general observation is carried out to the tension only and the non-symmetric models.

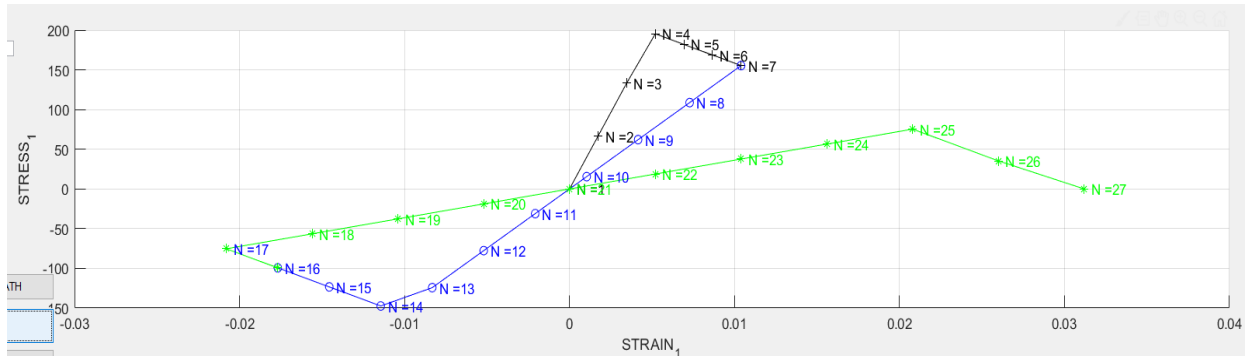


Figure 17: Stress vs. strain for the symmetric damage surface

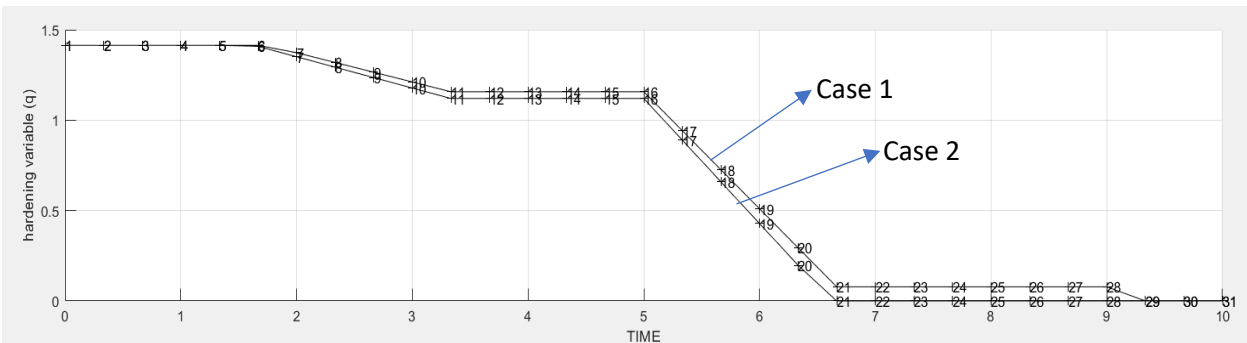


Figure 18: Hardening parameter(q) vs. time for the symmetric model (case 1 and case 3)

The tension only model is shown in Figure 19. The results are similar to the ones obtained in case 1. The behavior of the initial tension phase in black is similar for the tension only and the symmetric model. And the compressive phase in blue (overlaid by the green curve) is not subjected to any damage.

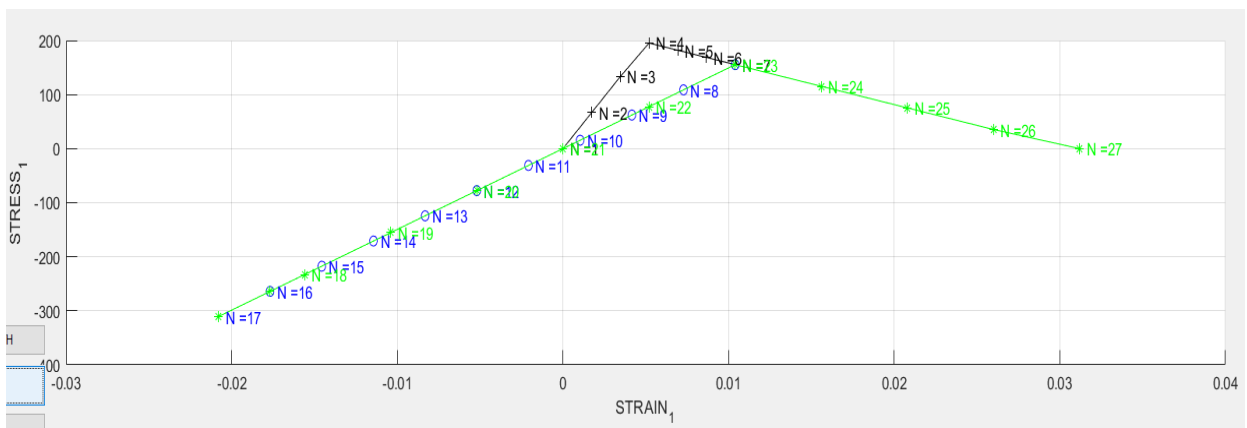


Figure 19: Stress vs. strain for the tension only damage surface

The non-symmetric model is shown in Figure 20. A ratio of 1.5 was used in order to ensure that damage occurs for all phases using the prescribed stresses. The results are similar to the ones obtained in case 1. A similar behavior to the symmetric model occurs. However, the value for the onset of damage in the blue compressive phase is 1.5 times larger than the one in the symmetric model.

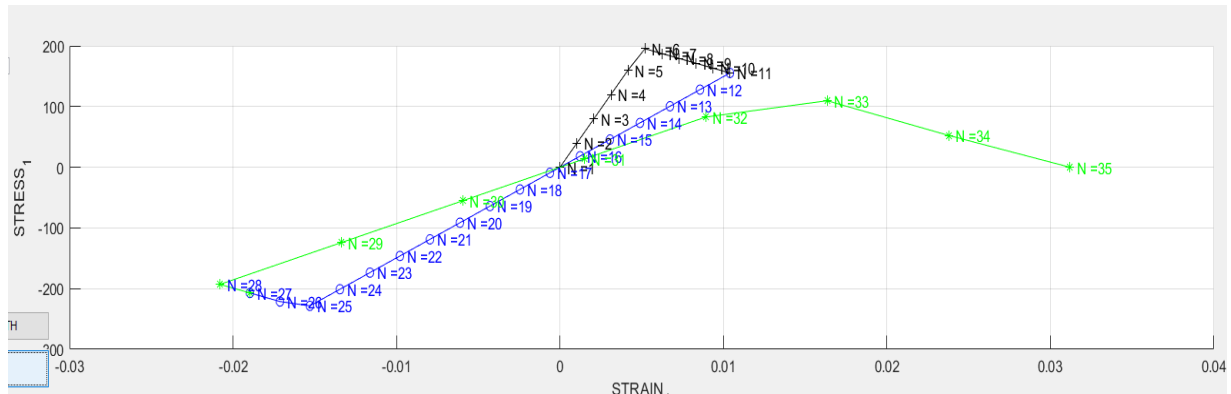


Figure 20: Stress vs. strain for the non-symmetric damage surface

## 2- VISCOUS (RATE DEPENDENT) MODEL

The second section of this report handles the implementation and evaluation of the correctness of the viscous damage model. In such a model, the effect of the viscosity is taken into account thus the results depend on the rate at which the loads are applied. Regarding the implementation of the model., only linear hardening law was implemented applied in the context of a symmetric elastic damage surface. Due to the time dependency of the problem in hand, a time integration scheme must be employed namely the alpha-method. The modifications to provided MATLAB code are shown in Appendix 2.

### 2-1 Assessing the correctness of the implementation

#### 2-2-1 Variation of the viscosity parameter $\eta$

In order to assess the correctness of the implementation, several testes were conducted. The first one being the modification of the viscosity parameter  $\eta$  in order to observe its effect on the stress/strain curve. A uniaxial tension only load was applied in order to ease the visualization. The material parameters are as follows:  $H = -0.1$ ,  $\alpha = 1$ ,  $\nu = 0.3$  and  $E = 2000$ . Alpha is set to 1 in order to recover the inviscid case when  $\eta$  tends to zero. The values used for  $\eta$  are as follows: 1, 0.8, 0.4 and 0. The result for the effect of this change on the stress strain curve is shown in Figure 21. This confirms that different behaviors for the stress/strain relation is obtained based of the value of the viscosity. In the present case of a softening regime, it could be observed that an increase in  $\nu$  results in a steeper decrease of the stress for the same value of strain.

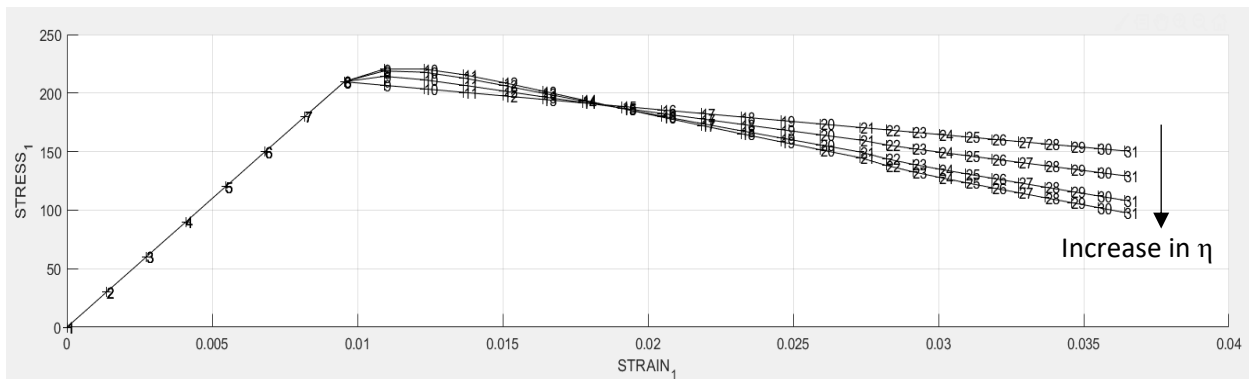


Figure 21: Stress vs. strain curves for  $\eta = 1, 0.8, 0.4$  and  $0$

It could be observed that when  $\alpha$  is set to 1 and  $\eta$  is set to zero, the inviscid case (Figure 22) is recovered.

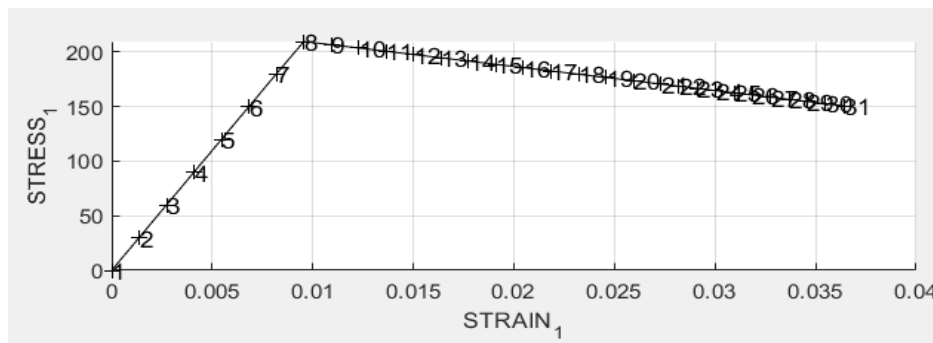


Figure 22: Stress strain curve for the same input parameters for the inviscid model

The time dependency of the results could be further illustrated using the evolution of stress with respect to time. It could be seen from Figure 23 that the inviscid case exhibits a linear behavior while the viscous case is nonlinear. Furthermore, the decrease in stress with respect to time is much steeper in the viscous case further justifying the results shown in Figure 21.

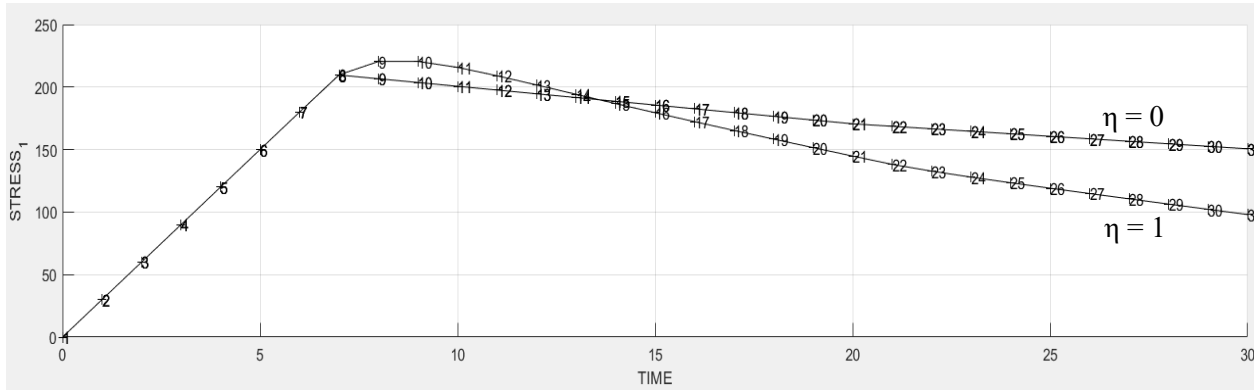


Figure 23: Stress vs. time for  $\eta = 0$  and  $1$

### 2-2-2 Variation of the strain rate $\dot{\epsilon}$

The second parameter to be analyzed is the strain rate  $\dot{\epsilon}$ . Its effect is to be observe its effect on the stress/strain curve. The input parameters are as follows:  $H = -0.1$ ,  $\nu = 0.5$ ,  $\alpha = 0.5$  and  $E = 2000$ . Th variation in strain rate is achieved by varying the total time giving it the following values: 5, 10, 15 and 20. This results in the decrease of the stain rate. The results are shown in Figure 24. It could be noted that the decrease in strain rate has a diminishing effect on the behavior of the stress/strain curve. At very low strain rate the stress/strain behavior of the inviscid model is recovered.

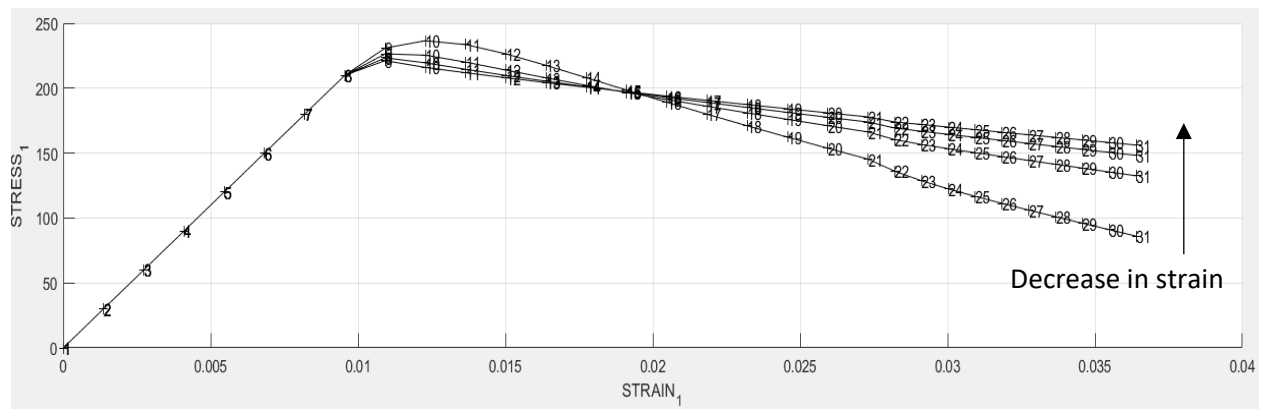


Figure 24: Stress vs. strain curve for different strain rates

### 2-2-3 Variation of the time integration parameter $\alpha$

The third parameter to be analyzed is the time integration parameter  $\alpha$ . Its effect is to be observe its effect on the stress/strain curve. This parameter affects the time integration scheme where a value of 0 employs an explicit scheme, a value of 0.5 employs a Crank-Nicolson scheme and a value of 1 employs an implicit

scheme. A uniaxial tension only load was applied in order to ease the visualization. The material parameters are as follows:  $H = -0.1$ ,  $\nu = 0.5$  and  $E = 2000$ . The results for the different values of  $\alpha$  are shown in Figure 25. It could be observed that the value of  $\alpha$  has a great effect on the obtained solution. This is due to the nature of the integration scheme itself. Where the explicit method is unstable beyond a certain threshold. The implicit method is unconditionally stable however its is not consistent i.e. the convergence to the correct solution is not assured. The Crank-Nicolson method is also unconditionally stable; however, it provides a quadratic scheme in time thus providing higher accuracy and convergence compared to the implicit method. All the scheme would tend to the same solution if a sufficiently fine discretization (in a finite element sense) is applied.

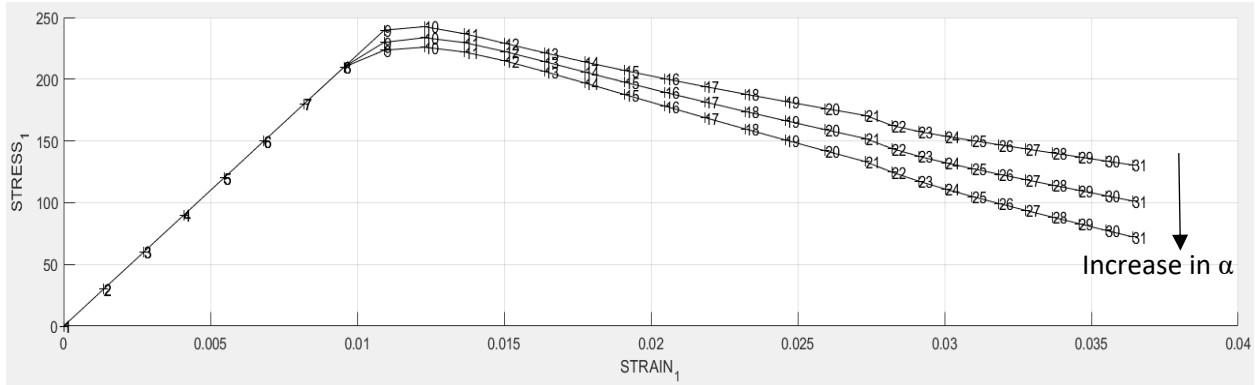


Figure 25: Stress vs. strain for  $\alpha = 0, 0.5$  and  $1$

## 2-2 Tangent and algorithmic constitutive operators $C_{11}$

In this section, the tangent and algorithmic constitutive operators are discussed. In a gauss point level, there is no difference in the implementation of either operators; however, the difference is more pronounced in a finite elements scheme. The constitutive operator specifies the relation between stress and strain. The constitutive algorithmic operator is computed when an incremental scheme for calculating the strains and stresses is used. The increment of stress is obtained based on the increment of strain. On the other hand, the tangent constitutive operator is used to compute the total stress from the total strain. This gives rise to different performance concerning the stability and the convergence of the solution. In general, the algorithmic tangent operator is easier to implement and provides a more robust method to obtain the solution.

In the case of the model in hand, the behavior of the  $C_{11}$  component of the algorithmic/tangent operator in time is to be analyzed for different values of the time integration parameter  $\alpha$ . The results are shown in Figure 26. It could be observed that an increase in the value of  $\alpha$  results in the steeper decrease of the value of the  $C_{11}$  component in the damaged region while the value remains constant in the elastic region.

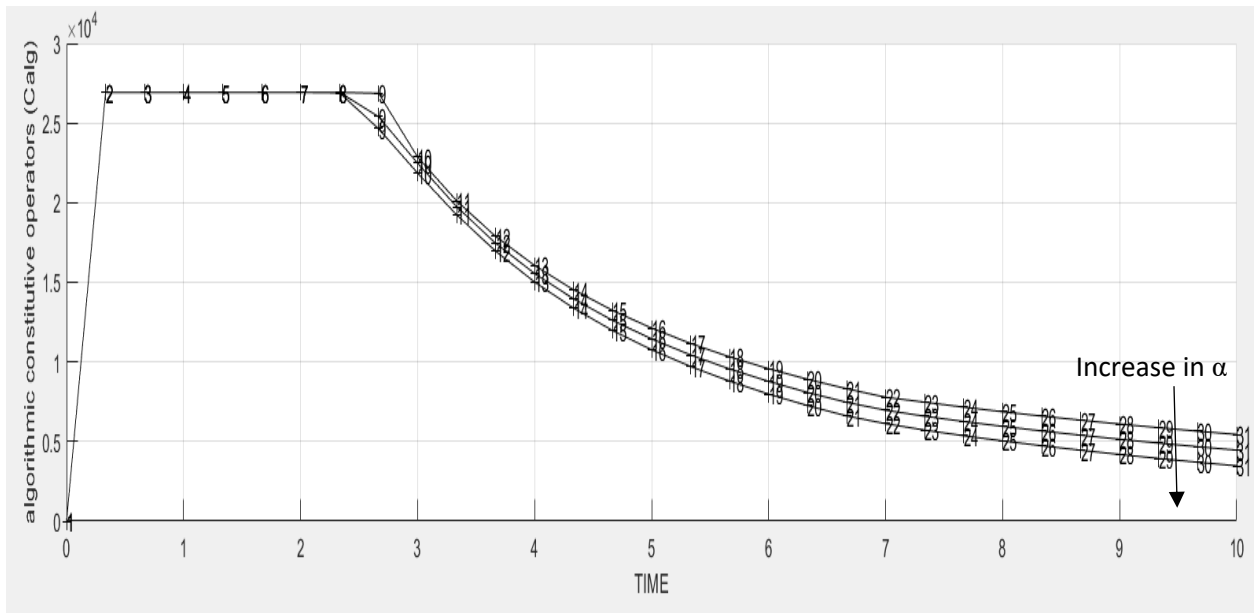


Figure 26: Constitutive algorithmic/tangent tensor vs. time for  $\alpha = 0, 0.5$  and  $1$

## APPENDIX

### Appendix 1-1

MATLAB code for the tension only elastic damage surface (modification to Mdelos\_de\_dano1)

```
elseif (MDtype==2)  %* Only tension

    sigm_p = [ mcau(sigm(1)) mcau(sigm(2)) mcau(sigm(3)) mcau(sigm(4)) ];
    rtrial = sqrt( sigm_p * eps );
```

MATLAB code for the non-symmetric elastic damage surface (modification to Mdelos\_de\_dano1)

```
elseif (MDtype==3)  %*Non-symmetric

    thet = ( mcau(sigm(1))+ mcau(sigm(2)) + mcau(sigm(4)) ) / (
abs(sigm(1))+ abs(sigm(2)) + abs(sigm(4)) ) ;
    z = thet + (1-thet)/n ;
    rtrial= z * sqrt(eps_n1*ce*eps_n1') ;
```

### Appendix 1-2

MATLAB code for exponential hardening (modification to rmap\_dano1)

```
else
    % Exponential %%%%%%%%%%%%%%%%%%%%%%%%%%%%%%%%%%%%%%%%%%%%%%%%%%%%%%%%%%%%%%%%%%%%%%%%%
    qinf = r0 + abs(r0-zero_q);
    A = (H * r0) / ( qinf - r0 );
    q_n1 = qinf - (qinf-q_n)*exp(A*(1-(rtrial/r_n)));
    % q_n + ( (delta_r*A*(qinf-r0) ) / (r0) ) * exp(A*(1-(rtrial/r0))) ;
```

### Appendix 2-1

MATLAB modification for viscous effects (modification to function calls)

```
function [sigma_n1,hvar_n1,aux_var] = rmap_dano1
(eps_n1,hvar_n,Eprop,ce,MDtype,n,strain,delta_t,eta)

function [rtrial] = Modelos_de_dano1 (MDtype,ce,eps_n1,n,Eprop,strain)

function
[sigma_v,vartoplot,LABELPLOT,TIMEVECTOR]=damage_main(Eprop,ntype,istep,strain
,MDtype,n,TimeTotal,eta)
```

## MATLAB modification for viscous effects (modification to rmap\_dano1)

```
if(rtrial > r_n)
    %* Loading

    fload=1;
    delta_r=rtrial-r_n;
    if Eprop(6) == 0
        r_n1 = rtrial ;
    else
        r_n1 = ( (eta-delta_t*(1-alpha))/(eta+alpha*delta_t) ) * r_n +
(delta_t/(eta+alpha*delta_t)) * rtrial; %%%%%%%%%%%%%%%
    end
```

## Appendix 2-2

### MATLAB modifications to implement the C tangent (modification to rmap\_dano1)

```
% Compute C alg
if Eprop(6) == 0
    c_alg_n1 = (1.d0-dano_n1)*ce ;
else
    c_alg_n1 = (1.d0-dano_n1)*ce + (alpha*delta_t/(eta+alpha*delta_t)) *
(1/rtrial) * ((H*r_n1-q_n1)/(r_n1)^2) * kron(sigm_n1_bar,sigm_n1_bar');
%%%%%%%%%%%%%%
end
```

### Modification to damage\_main

```
    vartoplot{i}(4) = c_alg_n1 (1,1); % algorithmic constitutive
operators (Calg)
```

### MATLAB modification for viscous effects (modification to function calls)

```
function [sigma_n1,hvar_n1,aux_var,c_alg_n1] = rmap_dano1
(eps_n1,hvar_n,Eprop,ce,MDtype,n,strain,delta_t,eta)
```

```
LABELPLOT = {'hardening variable (q)', 'internal variable (r)', 'damage
variable (d)', 'algorithmic constitutive operators (Calg)'};
```